Electronic structures and properties of copper, germanium, or tin-based MA/Pb-free perovskite halides

THE UNIVERSITY OF SHIGA PREFECTURE

Takeo Oku, Riku Okumura, Yu-Chen Kuo, Atsushi Suzuki
Department of Materials Science, The University of Shiga Prefecture, Japan

Contact information:
oku@mat.usp.ac.jp

Introduction

Perovskite halides with a typical composition of $CH_3NH_3PbI_3$ provide high photoconversion efficiencies and lightweight/flexible solar cells. Since the main element Pb is toxic, perovskites without Pb (Pb-free) should be developed from the viewpoint of natural environments and human health. In addition, methyl ammonium (CH_3NH_3, MA) is an unstable molecule in the crystal, and MA-free perovskites are also mandatory to improve their structural stabilities.

Purpose

The aim of the present study is to clarify the electronic structures and properties of Cu, Ge, or Sn-based MA/Pb-free perovskite halides using first principles calculations

References

R. Okumura, T. Oku, A. Suzuki, Chemical Physics Impact 8 (2024) 100534.
Y.-C. Kuo, T. Oku, A. Suzuki, I. Ono, R. Okumura, Hybrid Advances 5 (2024) 100174.

Ge- or Sn-based Pb-Free perovskites

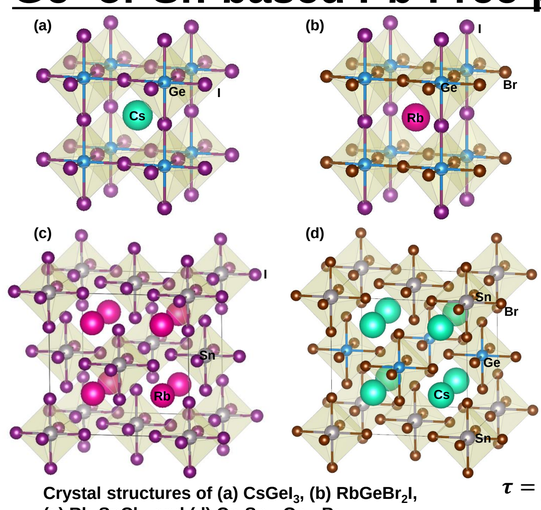

Crystal structures of (a) $CsGeI_3$, (b) $RbGeBr_2I$, (c) Rb_2SnCl_6, and (d) $Cs_2Sn_{0.5}Ge_{0.5}Br_6$.

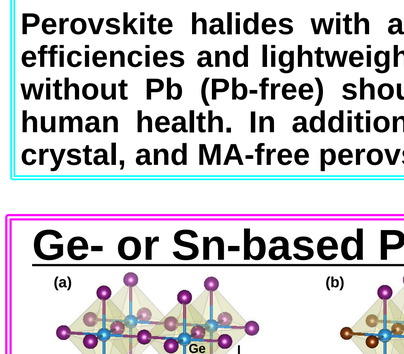

Relationship between tolerance factors and total energies.

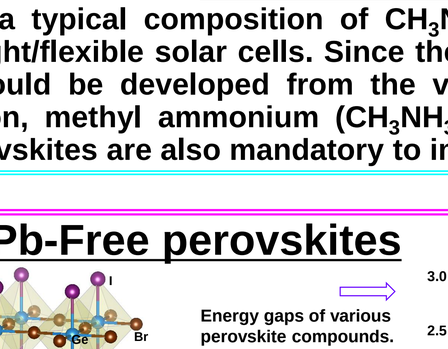

Calculated J-V characteristics of devices constructed with $CsSnCl_3$, Cs_2SnBr_6, and Cs_2SnI_6.

Calculated total energies, band gaps, optimized lattice constants, effective mass ratios, and t-factors of double perovskite structures.

Double perovskite	E_{tot} (eV·atom^{-1})	E_g (eV)	Transition	Lattice constants (Å)	m_h^*/m_0	m_e^*/m_0	t	τ
Cs_2SnI_6	-222.74	1.9810	Indirect	8.141/8.141/8.131	0.2463	0.0984	0.9217	4.2377
Cs_2GeI_6	-223.94	2.2140	Indirect	8.008/8.008/7.998	0.2640	0.0930	0.9846	3.9796
Cs_2SnBr_6	-258.57	1.2110	Direct	7.660	0.9103	0.1582	0.9395	3.8183
$Cs_2Sn_{0.5}Ge_{0.5}Br_6$	-259.17	0.8160	Direct	7.627/7.627/10.455	0.5255	0.0557	0.9732	4.7361
Cs_2GeBr_6	-259.75	0.6410	Direct	7.519	0.8596	0.1541	1.0094	4.4073
Cs_2SnCl_6	-286.86	2.4240	Direct	7.206	1.0205	0.1954	0.9523	4.2019
$Cs_2Sn_{0.5}Ge_{0.5}Cl_6$	-287.47	2.0910	Direct	7.166/7.166/9.997	2.5746	0.0747	0.9883	4.3734
Cs_2GeCl_6	-288.06	1.9080	Direct	7.096	1.0510	0.2050	1.0272	4.1153
Rb_2SnI_6	-222.79	1.9420	Indirect	8.114/8.114/8.111	5.4628	0.0957	0.8856	3.9540
Rb_2GeI_6	-223.94	2.1650	Indirect	7.969/7.969/7.960	6.8285	0.0906	0.9460	4.7629
Rb_2SnBr_6	-258.63	1.1370	Direct	7.578	0.8342	0.1448	0.9004	4.4341
$Rb_2Sn_{0.5}Ge_{0.5}Br_6$	-259.23	0.7180	Direct	7.546/7.546/10.258	0.4642	0.0500	0.9327	4.2287
Rb_2GeBr_6	-259.82	0.5310	Direct	7.401	0.7677	0.1358	0.9673	4.1087
Rb_2SnCl_6	-286.93	2.3310	Direct	7.052	0.8865	0.1682	0.9110	4.2764
$Rb_2Sn_{0.5}Ge_{0.5}Cl_6$	-287.54	1.9700	Direct	6.990/6.990/9.702	0.5255	0.0621	0.9455	4.5717
Rb_2GeCl_6	-288.14	1.7580	Direct	6.885	0.8418	0.1653	0.9827	4.2443

Energy gaps of various perovskite compounds.

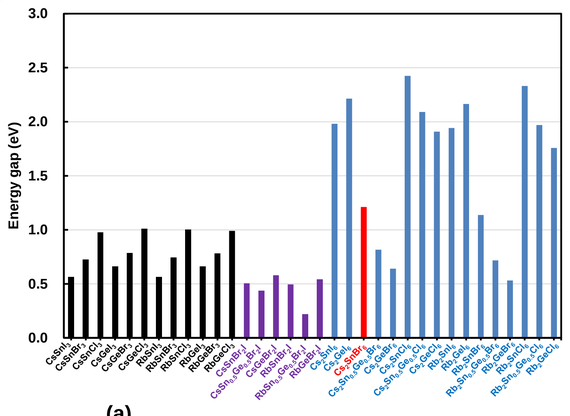

$$t = \frac{r_A + r_X}{\sqrt{2}(r_B + r_X)}$$

$$\tau = \frac{r_X}{r_B} - n_A\left[n_A - \frac{r_A/r_B}{\ln(r_A/r_B)}\right]$$

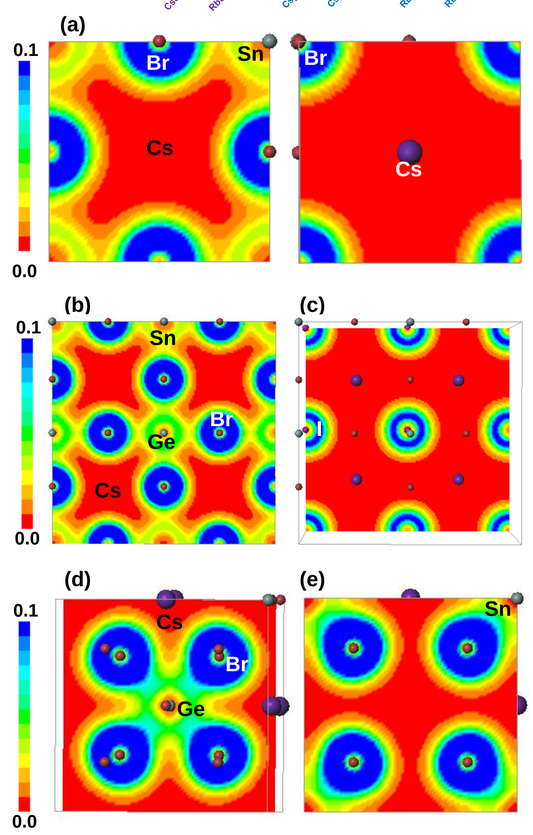

Electron density distributions of (a) $CsSnBr_3$ with different cross sections, (b, c) $CsSn_{0.5}Ge_{0.5}Br_2I$, and (d, e) $Cs_2Sn_{0.5}Ge_{0.5}Br_6$.

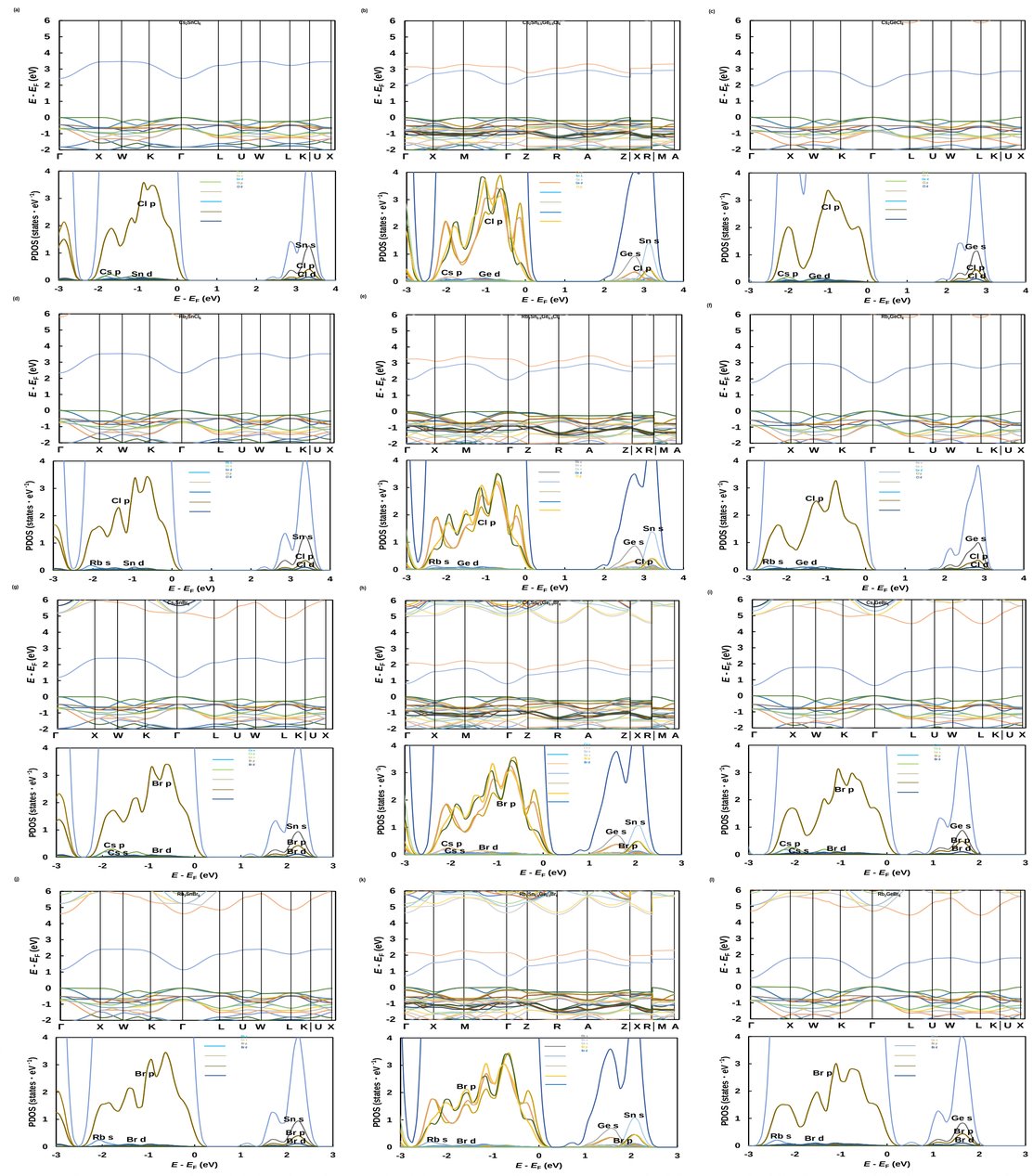

Band structures and partial density of states for (a) Cs_2SnCl_6, (b) $Cs_2Sn_{0.5}Ge_{0.5}Cl_6$, (c) Cs_2GeCl_6, (d) Rb_2SnCl_6, (e) $Rb_2Sn_{0.5}Ge_{0.5}Cl_6$, (f) Rb_2GeCl_6, (g) Cs_2SnBr_6, (h) $Cs_2Sn_{0.5}Ge_{0.5}Br_6$, (i) Cs_2GeBr_6, (j) Rb_2SnBr_6, (k) $RbSn_{0.5}Ge_{0.5}Br_6$, and (l) Rb_2GeBr_6 with double perovskite structures.

Cu-based MA-Free perovskites

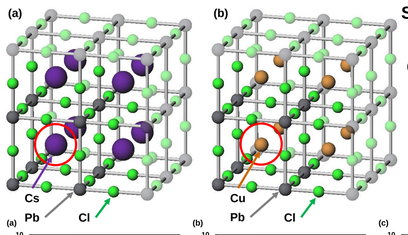

Structural models of (a) $CsPbCl_3$ and (b) $CuPbCl_3$

Crystal structures of reported ternary copper chlorides.

Compounds	Space group	Lattice constant (Å)
$CsPbCl_3$	Pm3m (221)	a = 5.6039(6)
Cu_2MnCl_4	Fm3m (225)	a = 5.3675(2)
Cu_2Cl_4	Fd3m (227)	a = 8.265
$CuCaCl_4$	P42c (112)	a = 5.415(1), c = 10.197(4)

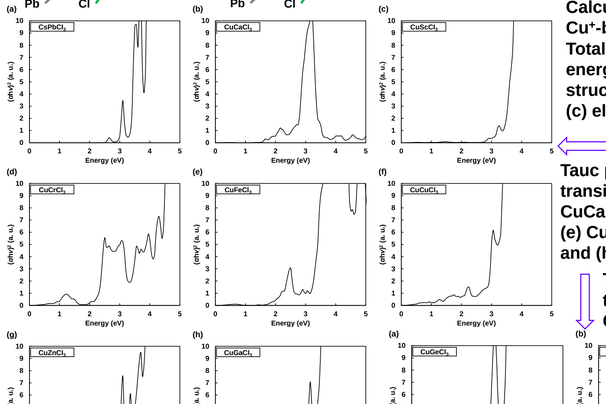

Tauc plots of direct allowed transitions for (a) $CsPbCl_3$, (b) $CuCaCl_3$, (c) $CuScCl_3$, (d) $CuCrCl_3$, (e) $CuFeCl_3$, (f) $CuCuCl_3$, (g) $CuZnCl_3$, and (h) $CuGaCl_3$.

Tauc plots of direct allowed transitions for (a) $CuGeCl_3$, (b) $CuSnCl_3$, and (c) $CuPbCl_3$.

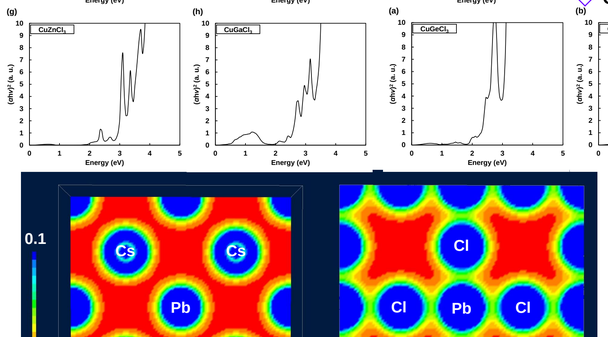

Electron density distributions on the cross sections of A-site (left) and $PbCl_6$ (right) for (a) $CsPbCl_3$ and (b) $CuPbCl_3$ crystals.

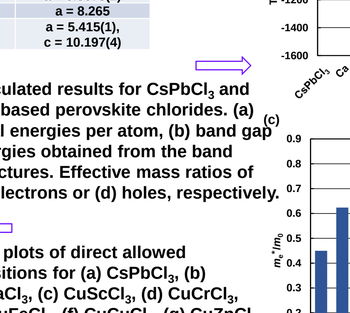

Calculated X-ray diffraction patterns of Cu+-based perovskite chlorides.

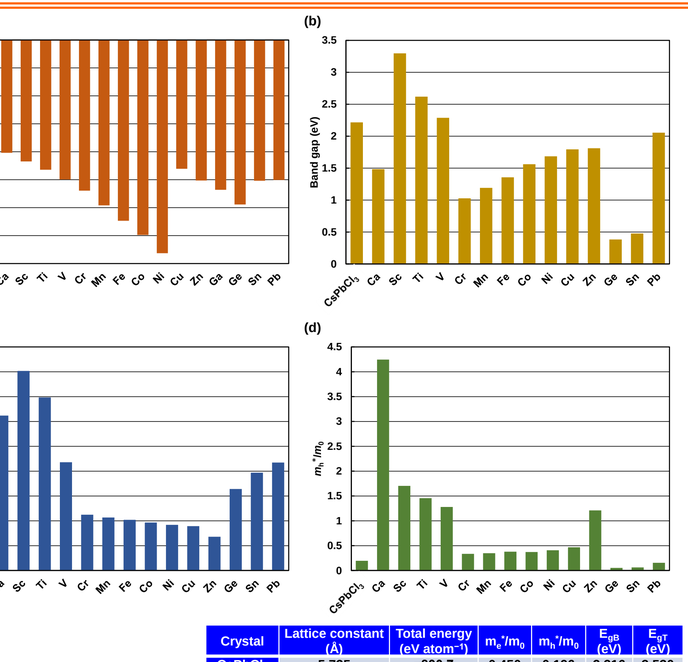

Calculated total energies, band gaps, effective mass ratios of electrons and holes, and band gaps for directly allowed transitions. E_{gB} and E_{gT} are band gap energies obtained from band structure or Tauc plots, respectively.

Crystal	Lattice constant (Å)	Total energy (eV atom^{-1})	m_e^*/m_0	m_h^*/m_0	E_{gB} (eV)	E_{gT} (eV)
$CsPbCl_3$	5.735	−830.7	0.450	0.196	2.216	2.530
$CuCaCl_3$	5.327	−807.2	0.624	4.245	1.484	1.536
$CuScCl_3$	5.052	−869.2	0.803	1.704	3.297	3.409
$CuTiCl_3$	4.891	−928.3	0.697	1.456	2.619	2.960
$CuVCl_3$	4.789	−998.1	0.436	1.279	2.288	2.759
$CuCrCl_3$	4.709	−1078.0	0.225	0.335	1.028	0.890
$CuMnCl_3$	4.675	−1183.6	0.213	0.349	1.192	1.075
$CuFeCl_3$	4.660	−1293.8	0.204	0.379	1.356	1.533
$CuCoCl_3$	4.611	−1395.0	0.193	0.374	1.561	1.783
$CuNiCl_3$	4.639	−1525.7	0.184	0.408	1.685	2.052
$CuCuCl_3$	4.756	−921.4	0.179	0.467	1.794	1.982
$CuZnCl_3$	4.850	−1005.7	0.136	1.211	1.812	2.229
$CuGaCl_3$	4.977	−1072.2	0.317	0.066	0.000	0.489
$CuGeCl_3$	5.098	−1177.1	0.520	1.793	1.911	1.861
$CuSnCl_3$	5.407	−1007.4	0.446	2.609	1.643	1.697
$CuPbCl_3$	5.586	−1001.6	0.435	0.156	2.055	1.844

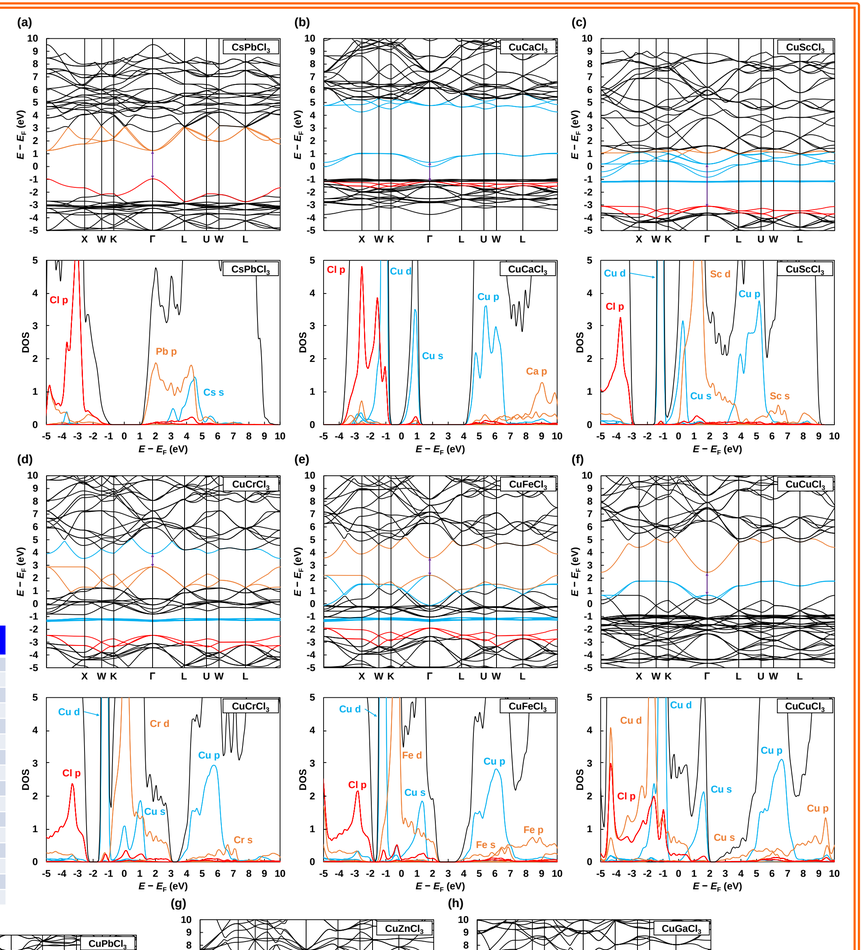

Calculated band structures and PDOS of (a) $CsPbCl_3$, (b) $CuCaCl_3$, (c) $CuScCl_3$, (d) $CuCrCl_3$, (e) $CuFeCl_3$, (f) $CuCuCl_3$, (g) $CuZnCl_3$, and (h) $CuGaCl_3$.

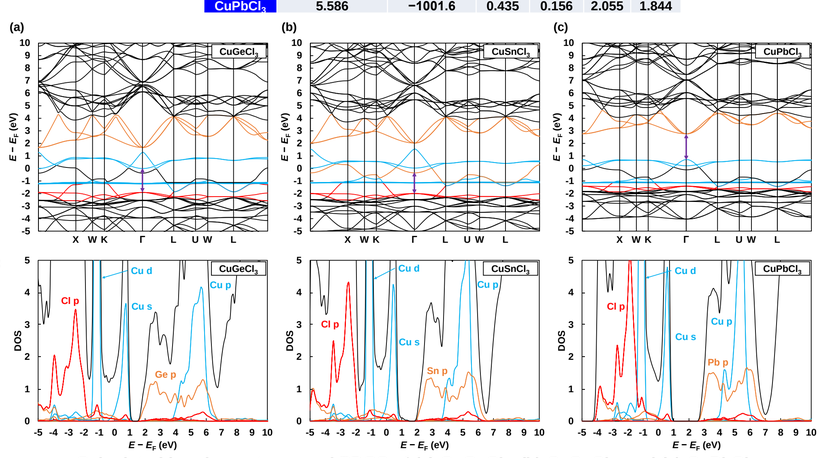

Calculated band structures and PDOS of (a) $CuGeCl_3$, (b) $CuSnCl_3$, and (c) $CuPbCl_3$.

Conclusion

Monovalent copper (Cu^+), rubidium (Rb), and cesium (Cs) were introduced at the MA sites, and various transition elements and typical elements such as Ni, Cr, Fe, Zn, and others were also induced at the Pb site. Pb-free double perovskite bromides were also found to be the suitable photovoltaic materials, which would be due to high electron density of Ge compared with Sn. The double perovskites have wide energy gaps and stabilities compared with the ordinary perovskites, and the hybridization of Ge/Sn would influence the electronic structures. Total energies of Cs-based perovskites were reduced by the Cu^+ addition. The band gap energies of Cu-based Pb-free chlorides with transition metals provided suitable values for solar cells. Carrier mobilities and crystal structures of the perovskites could be stabilized by overlapping of electron orbitals between the chloride octahedron and Cu^+. The Cu^+ at the MA-site would be effective to control the structures and stabilities of the all-inorganic perovskites, which would expand the multiplicity of the perovskites, and the α-formamidinium cesium lead triiodide was stably formed by the Cu^+ addition.